Single- and double-beta decay Fermi transitions in an exactly solvable model

Jorge G. Hirsch,[1,*] Peter O. Hess,[2,†] and Osvaldo Civitarese[3,‡]
[1]*Departamento de Física, Centro de Investigación y de Estudios Avanzados del IPN, Apdo. Postal 14-740, México 07000 Distrito Federal*
[2]*Instituto de Ciencias Nucleares, Universidad Nacional Autónoma de México, Apdo. Postal 70-543, México 04510 Distrito Federal*
[3]*Departamento de Física, Universidad Nacional de La Plata, c.c. 67 1900, La Plata, Argentina*
(Received 13 December 1996)

An exactly solvable model suitable for the description of single- and double-beta decay processes of the Fermi type is introduced. The model is equivalent to the exact shell-model treatment of protons and neutrons in a single-j shell. Exact eigenvalues and eigenvectors are compared to those corresponding to the Hamiltonian in the quasiparticle basis (qp) and with the results of both the standard quasiparticle random phase approximation (QRPA) and the renormalized one (RQRPA). The role of the scattering term of the quasiparticle Hamiltonian is analyzed. The presence of an exact eigenstate with zero energy is shown to be related to the collapse of the QRPA. The RQRPA and the qp solutions do not include this zero-energy eigenvalue in their spectra, probably due to spurious correlations. The meaning of this result in terms of symmetries is presented. [S0556-2813(97)03507-3]

PACS number(s): 21.60.Fw, 21.60.Jz, 23.40.Hc

I. INTRODUCTION

In the last years the study of the quasiparticle random phase approximation (QRPA) and its extensions, like the renormalized quasiparticle random phase approximation (RQRPA), have received renewed attention. The goal was to improve substantially the reliability of the QRPA description of nuclear double-beta decay transitions and, at the same time, to enhance the predictive power of the theory in an unambiguous way.

The predictive power of the QRPA, mostly in dealing with the calculation of the matrix elements for ground-state to ground-state two-neutrino double-beta decay transitions ($\beta\beta_{2\nu}$), is questionable since these amplitudes are extremely sensitive to details of the nuclear two-body interaction [1–4].

The inclusion of renormalized particle-particle correlations in the QRPA matrix amounts to a drastic suppression of the $\beta\beta_{2\nu}$-matrix elements. However, for some critical values of the model parameters, i.e., the renormalized two-body interactions, the otherwise purely real QRPA eigenvalue problem becomes complex. As a consequence of it the standard properties of the QRPA metric and conservation rules are severely downplayed by the appearance of strong ground-state correlations which jeopardize the stability of the theory. The most notorious example of this behavior, of the QRPA approach, is the calculation of the $\beta\beta_{2\nu}$ decay of ^{100}Mo [1,2,5–7].

The renormalized version of the QRPA (RQRPA) [8,9], which includes some corrections beyond the quasiboson approximation, has been recently reformulated [10] and applied to the $\beta\beta_{2\nu}$ decay problem [11]. Contrary to the QRPA, the RQRPA does not collapse for any value of the residual two-body interaction. Based on its properties, the RQRPA was presented as a cure for the instabilities of the QRPA and it was applied to calculations of the $\beta\beta_{2\nu}$ decay of ^{100}Mo [11]. Similar studies have been performed in the framework of the RQRPA and with the inclusion of proton-neutron pairing correlations in symmetry breaking Hamiltonians [12].

In a recent paper [13] we have shown that the RQRPA violates the Ikeda sum rule and that this violation is indeed present in many extensions of the QRPA. The study was based on the schematic proton-neutron Lipkin model.

In a subsequent work [14] we have introduced an exactly solvable model for the description of single- and double-beta decay Fermi-type transitions. This model is equivalent to a single-j shell model for protons and neutrons. The appearance of an eigenvalue at zero energy, in the exact spectrum, was found. Moreover, it has been shown that the presence of this zero-energy eigenvalue should be associated to the collapse of the QRPA. It was shown that the RQRPA does not include this zero-energy mode in its spectrum. It was also shown that the absence of this zero-energy state, in the RQRPA, leads to finite but spurious results for the transition amplitudes near the point of collapse of the QRPA.

In the present paper we discuss the details of the exactly solvable model of [14]. The algebraic techniques needed to evaluate matrix elements of the relevant operators, in the SO(5) group representation, are described in detail. Exact eigenvalues and eigenvectors are compared with those corresponding to the quasiparticle version of the Hamiltonian (qp) and with the ones obtained with the QRPA and RQRPA. The role of the correlations induced by the scattering term H_{31} of the qp Hamiltonian and the effects on the number of quasiparticles in the ground state are analyzed. The presence of a zero excitation energy state in the spectrum corresponding to the exact solution of the model Hamiltonian is discussed. As said before it will be shown that the RQRPA and the qp solutions do not display the same feature, most likely due to the presence of spurious states caused by the mixing of orders, of the relevant interaction terms, in the expansion procedure.

*Electronic address: hirsch@fis.cinvestav.mx
†Electronic address: hess@roxanne.nuclecu.unam.mx
‡Electronic address: civitare@venus.fisica.unlp.edu.ar

The structure of the paper is the following: the model and its solutions are presented in Sec. II, the quasiparticle version of the Hamiltonian, its linear representation in terms of pairs of unlike (proton-neutron) quasiparticle pairs and its properties are introduced in Sec. III. The QRPA and RQRPA treatments of the Hamiltonian are discussed in Sec. IV. The matrix elements of double-beta decay transitions, calculated in the framework of the different approximations introduced in the previous sections, are given in Sec. V. Conclusions are drawn in Sec. VI. The SO(5) algebra, representations and reduced matrix elements used in the calculations are given in detail in Appendices A, B, and C, respectively.

II. THE MODEL

The model Hamiltonian, which includes a single-particle term, a pairing term for protons and neutrons, and a schematic charge-dependent residual interaction with both particle-hole and particle-particle channels, has been introduced in [15–17] and it is given by

$$H = e_p \mathcal{N}_p - G_p S_p^\dagger S_p + e_n \mathcal{N}_n - G_n S_n^\dagger S_n + 2\chi \beta^- \cdot \beta^+ - 2\kappa P^- \cdot P^+, \tag{1}$$

with

$$\mathcal{N}_i = \sum_{m_i} a_{m_i}^\dagger a_{m_i}, \quad S_i^\dagger = \sum_{m_i} a_{m_i}^\dagger a_{\bar{m}_i}^\dagger / 2, \quad i = p,n,$$

$$\beta^- = \sum_{m_p = m_n} a_{m_p}^\dagger a_{m_n}, \quad P^- = \sum_{m_p = -m_n} a_{m_p}^\dagger a_{\bar{m}_n}^\dagger, \tag{2}$$

$a_p^\dagger = a_{j_p m_p}^\dagger$ being the particle creation operator and $a_{\bar{p}}^\dagger = (-1)^{j_p - m_p} a_{j_p - m_p}^\dagger$ its time reversal. The parameters χ and κ play the role of the renormalization factors g_{ph} and g_{pp} introduced in the literature [1–4].

It has been shown in a series of papers [17–19] that this Hamiltonian, when treated in the framework of the QRPA, reproduces fairly well the results obtained with a realistic G matrix constructed from the Bonn-OBEP potential, both for single- and double-beta decay transitions. These results can be taken as an indication about the correlations induced by the interactions in Eq. (1), which are obviously specific to the relevant degrees of freedom of the problem. In other words, if the relatively simple schematic force (1) can approximately describe the correlations induced by a more realistic interaction it certainly means that it is able to pick up the bulk of the physics involved in the transitions.

In a single-one-shell limit, for the model space ($j_p = j_n = j$) and for monopole ($J = 0$) excitations, the Hamiltonian (1) can be solved exactly. In spite of the fact that the solutions obtained in this restricted model space cannot be related to actual nuclear states, the excitation energies, single- and double-beta decay transition amplitudes, and ground-state correlations depend on the particle-particle strength parameter κ in the same way as they do in realistic calculations with many single-particle levels and with more realistic interactions, as we shall show later on. Physically, the beta decay transitions between $J^\pi = 0^+$ states correspond to transitions of the Fermi type. However, the study of the model and the identification of its relevant degrees of freedom, instead of the comparison of observables, is the main aspect of the present work. We shall obtain the eigenstates of Eq. (1), by using different approximations, in order to build up a comprehensive view about the validity of them and their predictive power.

The Hamiltonian (1) can be expressed in terms of the generators of an SO(5) algebra [20–22]. The Hilbert space is constructed by using the eigenstates of the particle-number operator $\mathcal{N} = \mathcal{N}_p + \mathcal{N}_n$, the isospin $\mathcal{T}$, and its projection $\mathcal{T}_z = (\mathcal{N}_n - \mathcal{N}_p)/2$. The raising and lowering isospin operators are defined as $\beta^\pm = \mathcal{T}^\pm$, where $\mathcal{T}^- |n\rangle = |p\rangle$. With them we can construct the isospin scalar $\mathcal{T}^2 = \frac{1}{2}(\mathcal{T}^- \mathcal{T}^+ + \mathcal{T}^+ \mathcal{T}^-) + \mathcal{T}_z^2$ and the second-order SO(5) Casimir (see Appendix A):

$$S_n^\dagger S_n + S_p^\dagger S_p + \frac{1}{2} P^\dagger P = \frac{\mathcal{N}}{4}\left(3 - \frac{\mathcal{N}}{2} + 2\Omega\right) - \frac{\mathcal{T}}{2}(\mathcal{T}+1) \tag{3}$$

with $\Omega = (2j+1)/2$.

The Hamiltonian (1) can be expressed in terms of the above-mentioned operators. Hereafter we will use $G_p = G_n \equiv G$ for simplicity. In terms of these generators the Hamiltonian (1) reads

$$H = \left[e_p + e_n - \frac{1}{3}\left(3 + 2\Omega - \frac{\mathcal{N}}{2}\right)(G + 2\kappa)\right]\frac{\mathcal{N}}{2} + [e_n - e_p - 2\chi(\mathcal{T}_z - 1)]\mathcal{T}_z + \left[2\chi + \frac{G}{3} + \frac{2}{3}\kappa\right]\mathcal{T}(\mathcal{T}+1) + \sqrt{\frac{2}{3}}\Omega(4\kappa - G)[[a^\dagger a^\dagger]^{J=0,\mathcal{T}=1}[aa]^{J=0,\mathcal{T}=1}]^{\mathcal{T}=2}_{\mathcal{T}_z=0}. \tag{4}$$

In writing the creation and annihilation operators ($a^\dagger$, a) we have omitted unnecessary subindexes since the coupling to total angular momentum J and isospin $\mathcal{T}$, represented as $[a^\dagger a^\dagger]^{J,\mathcal{T}}$, is understood.

Hamiltonian (5) is diagonal in the $\mathcal{N},\mathcal{T},\mathcal{T}_z$ basis if $G = 4\kappa$. It can be reduced to an isospin scalar if its parameters are selected as

$$e_p = e_n, \quad \chi = 0, \quad G = 4\kappa. \tag{5}$$

If $4\kappa \neq G$ the Hamiltonian (1) is not diagonal in this basis. The Hamiltonian mixes states with different isospin T while its eigenstates still have definite N and T_z. The dynamical breaking of the isospin symmetry is an essential aspect of the model which is directly related to the nuclear structure

mechanism responsible for the suppression of the matrix elements for double-beta decay transitions.

A. The diagonal case $G=4\kappa$

The solution of Eq. (1) in the basis $|\mathcal{N},\mathcal{T},\mathcal{T}_z\rangle$, in the case $G=4\kappa$, gives a state, the isobaric analog state (IAS) at the energy

$$E_{\rm IAS}=E(\mathcal{N},\mathcal{T},\mathcal{T}_z=\mathcal{T}-1)-E(\mathcal{N},\mathcal{T},\mathcal{T}_z=\mathcal{T})$$
$$=e_p-e_n+4\chi(\mathcal{T}-1). \quad (6)$$

Considering a double Fermi transition, the energy available for the decay is given by

$$E_{\beta\beta}=E(\mathcal{N},\mathcal{T},\mathcal{T}_z)-E(\mathcal{N},\mathcal{T}',\mathcal{T}'_z)$$
$$=2(e_n-e_p)+8\chi+G(2\mathcal{T}-1) \quad \text{if } \mathcal{T}\geqslant 2, \quad (7)$$

where $\mathcal{T}'_z=\mathcal{T}_z-2$. The above expression shows clearly the role of the particle-hole strength parameter χ. It determines the excitation energy of the IAS, which depends not only upon the proton-neutron energy shift due to the nuclear Coulomb field but also upon χ and $\mathcal{T}$. The same dependence is shown by the $Q_{\rm value}$ [Eq. (7)]. In analogy with the situation found in realistic calculations its value can be determined by a fit to the experimental value of the IAS energy (or to the Gamow-Teller giant resonance for the case of $J^\pi=1^+$ spin-isospin-dependent excitations).

The β decay operators for single Fermi transitions, $\mathcal{T}^\pm$, do not change the total isospin or the total particle number of the state upon which they act. Only the isospin projection of the state is changed in steps of one unit, namely,

$$\mathcal{T}^\pm|\mathcal{N}\mathcal{T}\mathcal{T}_z\rangle=\sqrt{(\mathcal{T}\pm\mathcal{T}_z+1)(\mathcal{T}\mp\mathcal{T}_z)}|\mathcal{N}\mathcal{T}\mathcal{T}_z\pm 1\rangle. \quad (8)$$

B. The spectrum

For the numerical examples we have selected $N_n>N_p$ and a large value of j to simulate the realistic situation found in medium- and heavy-mass nuclei. To perform the calculations we have adopted the following two sets of parameters:

set I: $j=9/2$, $N=10$, $0\leqslant T_z\leqslant 4$,
$e_p=0.96$ MeV, $e_n=0.0$ MeV,
$G_p=G_n=0.4$ MeV, $\chi=0$ or 0.04 MeV, $0\leqslant\kappa\leqslant 0.2$,

and

set II: $j=19/2$, $N=20$, $1\leqslant T_z\leqslant 5$,
$e_p=0.69$ MeV, $e_n=0.0$ MeV,
$G_p=G_n=0.2$ MeV, $\chi=0$ or 0.025 MeV, $0\leqslant\kappa\leqslant 0.1$.

The dependence of the spectrum and transition matrix elements on the parameters χ and κ is analyzed in the following paragraphs.

The complete set of 0^+ states, belonging to different isotopes, is shown in Fig. 1(a) and Fig. 2(a), for $G=4\kappa$ and $\chi=0$, as a function of the number of protons (Z). The states are labeled by the isospin quantum numbers (T,T_z). Ground states are shown by thicker lines. As shown in these figures the structure of the mass parabola is qualitatively reproduced.

The upper insert, (a) of each figure, shows the full spectrum corresponding to $\chi=0$. The lower one, (b), shows the results corresponding to $\chi=0.05$ MeV [Fig. 1(b)] and $\chi=0.025$ MeV in [Fig. 2(b)]. Obviously the particle-hole channel of the residual interaction stretches the spectra of all isotopes. As mentioned above, it increases the energy of the IAS.

Beta decay transitions of the Fermi type, mediated by the action of the operator $\beta^-=t^-$, are allowed between states belonging to the same isospin multiplet. The energy of each member of a given multiplet increases linearly with Z.

In this example the 0^+ states belonging to each odd-odd-mass nuclei $(N-1,\ Z+1,\ A)$ are the IAS constructed from the 0^+ states of the even-even-mass nuclei with (N,Z,A) nucleons. Thus, Fermi transitions between them are allowed.

Since the isospin of the ground state of each of the even-even-mass nuclei differs, for different isotopes, Fermi double-beta decay transitions connecting them are forbidden in this diagonal limit $G=4\kappa$.

C. Exact solutions

The Hamiltonian (1) has a $\mathcal{T}=2$ tensorial component which mixes states with different isospins, while particle number and isospin projection remain as good quantum numbers.The diagonalization of Eq. (1) is performed in the basis of states described in Appendix B. The corresponding reduced matrix elements are given in Appendix C. The eigenstates are written as

$$|\mathcal{N}\mathcal{T}_z\alpha\rangle=\sum_{\mathcal{T}} \mathcal{C}^{\alpha}_{\mathcal{N}\mathcal{T}\mathcal{T}_z}|\mathcal{N}\mathcal{T}\mathcal{T}_z\rangle. \quad (9)$$

The energy of the ground state $(0^+_{\rm g.s.})$ and of the first-excited state (0^+_1), as a function of the ratio $4\kappa/G$ for the set of parameters $j=9/2$, $\mathcal{N}_n=6$, $\mathcal{N}_p=4$, $\chi=0$ are shown in

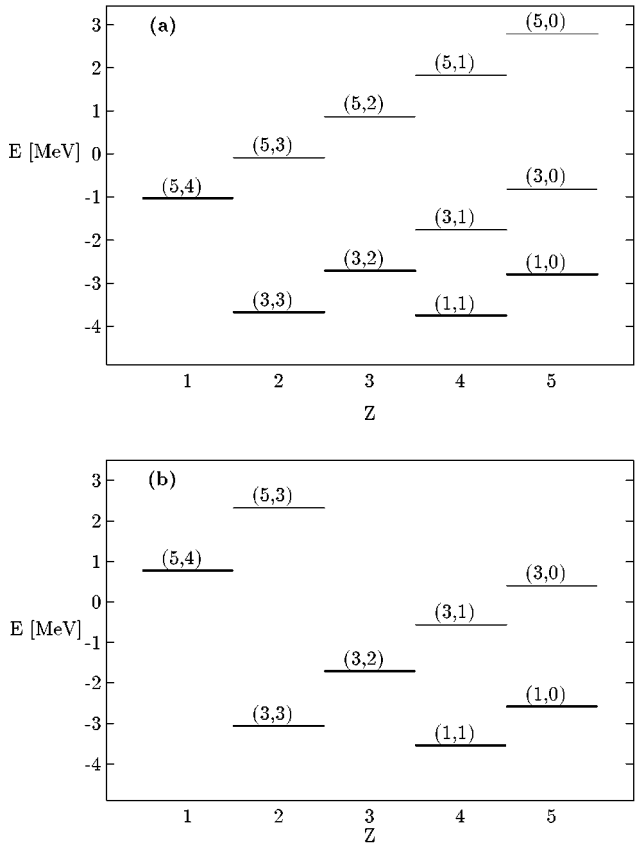

FIG. 1. (a) and (b): 0^+ states of different isotopes are shown for $j=9/2$, $4\kappa/G=1$, and $\chi=0.(0.05)$ MeV in an energy vs Z plot. States are labeled by (T,T_z). The lowest energy state of each nucleus is shown by a thick line.

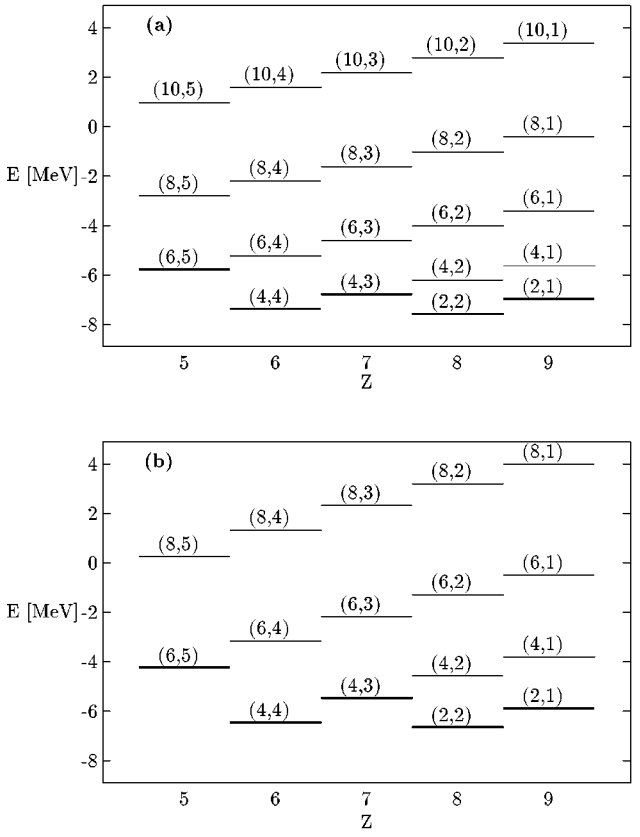

FIG. 2. (a) and (b): The same as Fig. 1 for $j=19/2$, $4\kappa/G=1$, and $\chi=0$ (0.025) MeV.

Fig. 3(a). The results of Fig. 3(b) have been obtained with the set of parameters given by $j=19/2$, $\mathcal{N}_n=12$, $\mathcal{N}_p=8$, and $\chi=0$.

The most characteristic feature of the results is the barely avoided crossing of levels, due to the repulsive nature of the effective residual interaction between them. Although a complete level crossing is not obtained in this model, in the neighborhood of the value $4\kappa/G\approx1$ a major structural change in the wave functions will develop. In the case of a complete crossing of levels, the ground and the first excited states will interchange their quantum numbers thus giving rise to a permanently deformed (in the sense of the isospin dominance) situation.

This behavior is by no means a surprise since it is similar to that found in pairing plus quadrupole systems [23]. In this case, if the quadrupole-quadrupole interaction is strong enough, the system becomes permanently deformed, in the sense of the angular momentum and spatial rotations. The analogy between this and the present case (isospin degree of freedom) can be drawn from the study of [24,25] where the ''pairing plus monopole'' model, which is a two-level model exactly solvable using the SO(5) algebra, was used to analyze the spherical and the deformed regime of the solutions of the multipole-multipole interaction.

The full-thin line of Fig. 4(a) [Fig. 4(b)] represents the excitation energy $E_{\rm exc}$ of the lowest 0^+ state belonging to the double-odd-mass nucleus ($\mathcal{N}_n=7,\mathcal{N}_p=3$) with respect to the parent even-even-mass nucleus ($\mathcal{N}_n=8,\mathcal{N}_p=2$) as a function of the ratio $4\kappa/G$ for $j=9/2$ and $\chi=0$ (0.04). It is clear that when $4\kappa/G\approx1.6$ (1.8) an attractive proton-neutron correlation dominates over proton-proton and neutron-neutron pairing correlations and the excitation energy goes to zero. Similar results are depicted in Figs. 5(a) and 5(b), corresponding to the excitation energy $E_{\rm exc}$ of the lowest 0^+ state in the odd-odd mass nucleus ($\mathcal{N}_n=13$, $\mathcal{N}_p=7$), also measured from the ground state of the parent even-even nucleus with ($\mathcal{N}_n=14,\mathcal{N}_p=6$) for $j=19/2$ and $\chi=0$ (0.025). In the case of Fig. 5 the excitation energy goes to zero when $4\kappa/G\approx1.3$.

The vanishing of the energy of the first excited state and the subsequent inversion of levels (or negative excitation energies) would indicate that the double-odd nucleus becomes more bound than their even-even neighbors, contradicting the main evidence for the dominance of like nucleons pairing in medium- and heavy-mass nuclei. It would also completely suppress the double-beta decay because the single-beta decay from each ''side'' of the double-odd nucleus would be allowed.

These results simply emphasize the fact that the Hamiltonian (1) will not be the adequate one when attractive proton-neutron interactions are too large. In a realistic situation, obviously, the true Hamiltonian includes other degrees of freedom, like quadrupole-quadrupole interactions, and permanent deformations of the single-particle mean field can also be present. These additional degrees of freedom will prevent the complete crossing of levels which, of course, is not observed. However, in many cases the experimentally observed energy shift of double-odd-mass nuclei with re-

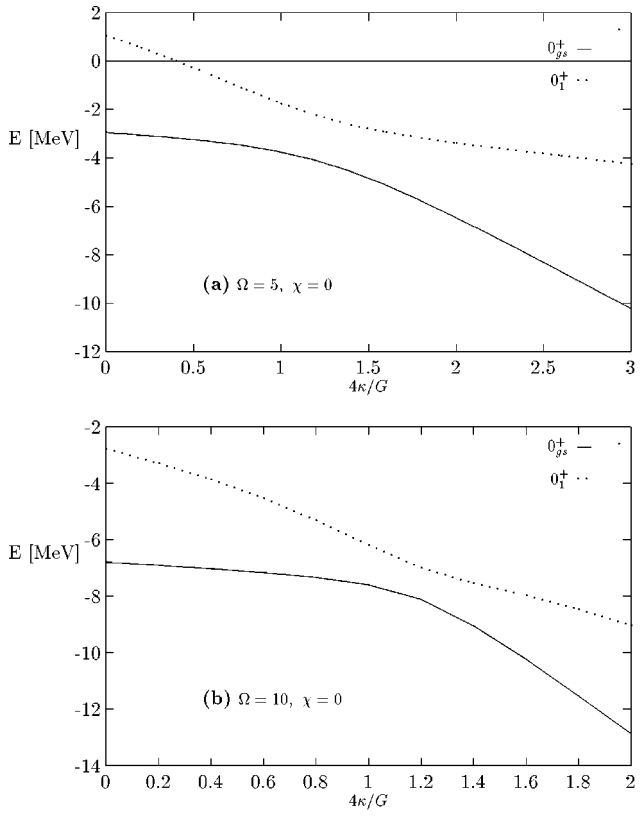

FIG. 3. (a) Energy of the ground state $0^+_{\text{g.s.}}$ (full line) and first excited state 0^+_1 (dotted line), as a function of the ratio $4\kappa/G$, for $j=9/2$, $\mathcal{N}_n=6$, $\mathcal{N}_p=4$, $\chi=0$. (b) Shows the same quantities for $j=19/2$, $\mathcal{N}_n=12$, $\mathcal{N}_p=8$.

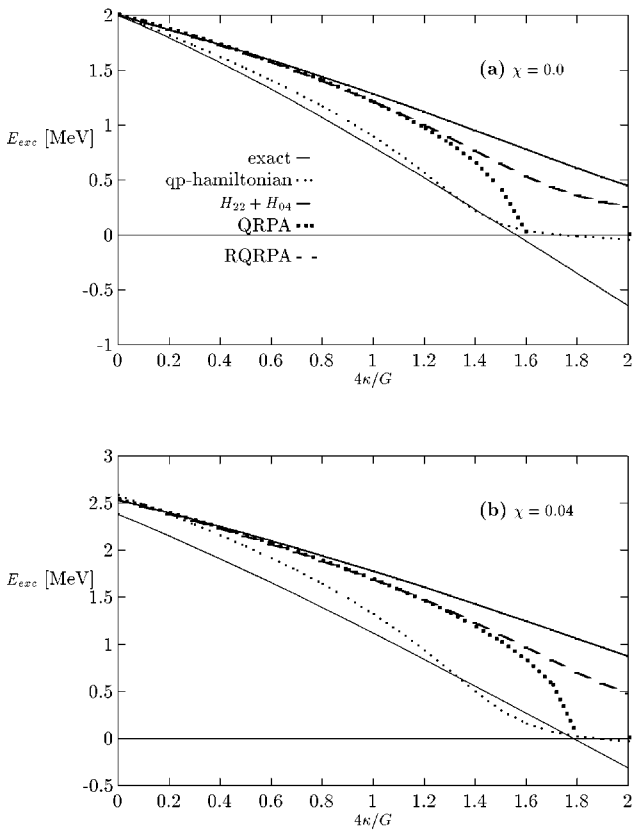

FIG. 4. (a) and (b): Excitation energy E_{exc} of the lowest 0^+ state in the odd-odd intermediate nucleus ($\mathcal{N}_n=7,\mathcal{N}_p=3$) with respect to the parent even-even nucleus ($\mathcal{N}_n=8,\mathcal{N}_p=2$) against $4\kappa/G$ for $j=9/2$, $\chi=0$ (0.04). Exact results are shown as thin-full lines while those of the qp Hamiltonian are shown as small-dotted lines. Results corresponding to the linearized qp Hamiltonian are shown as full-thick lines and the results obtained with the QRPA and RQRPA methods as large-dotted and dashed lines, respectively.

spect to their double-even-mass neighbors is very small. This finding reinforces the notion of an underlying dynamical-symmetry-restoration effect.

III. THE HAMILTONIAN IN THE QUASIPARTICLE (qp) BASIS

By performing the transformation of the particle creation and annihilation operators of the Hamiltonian (1) to the quasiparticle representation [26]; i.e., by using the Bogolyubov transformations for protons and neutrons, we have obtained the Hamiltonian

$$\begin{aligned} H=&(\epsilon_p-\lambda_p)N_p+(\epsilon_n-\lambda_n)N_n+\lambda_1A^\dagger A+\lambda_2(A^\dagger A^\dagger+AA)\\ &-\lambda_3(A^\dagger B+B^\dagger A)-\lambda_4(A^\dagger B^\dagger+BA)+\lambda_5B^\dagger B\\ &+\lambda_6(B^\dagger B^\dagger+BB), \end{aligned} \tag{10}$$

where ϵ_p,ϵ_n are the quasiparticle energies, λ_p,λ_n the chemical potentials, and

$$A^\dagger=[\alpha^\dagger_p\otimes\alpha^\dagger_n]^{J=0}_{M=0},\quad B^\dagger=[\alpha^\dagger_p\otimes\alpha^\dagger_{\bar{n}}]^{J=0}_{M=0},$$

$$N_i=\sum_{m_i}\alpha^\dagger_{im_i}\alpha_{im_i}\quad i=p,n$$

$$\lambda_1=4\Omega[\chi(u_p^2v_n^2+v_p^2u_n^2)-\kappa(u_p^2u_n^2+v_p^2v_n^2)],$$

$$\lambda_2=4\Omega(\chi+\kappa)u_pv_pu_nv_n, \tag{11}$$

$$\lambda_3=4\Omega(\chi+\kappa)u_nv_n(u_p^2-v_p^2),$$

$$\lambda_4=4\Omega(\chi+\kappa)u_pv_p(u_n^2-v_n^2),$$

$$\lambda_5=4\Omega[\chi(u_p^2u_n^2+v_p^2v_n^2)-\kappa(u_p^2v_n^2+v_p^2u_n^2)],$$

$$\lambda_6=-\lambda_2.$$

The operators $A^\dagger$ (A), which create (annihilate) a pair of unlike (proton and neutron)-quasiparticles, together with their counterparts for pairs of identical quasiparticles and $B,B^\dagger,N_p,N_n$ are the generators of the SO(5) algebra [20].

The quasiparticle energies

$$\epsilon=G\Omega/2 \tag{12}$$

and the occupation probabilities

$$v_p^2=\frac{\mathcal{N}_p}{2}j+1,\quad v_n^2=\frac{\mathcal{N}_n}{2j+1} \tag{13}$$

are determined from the gap equations and particle-number conservation condition [26]. The occupation probabilities can also be defined in terms of the single-particle and quasiparticle energy, namely:

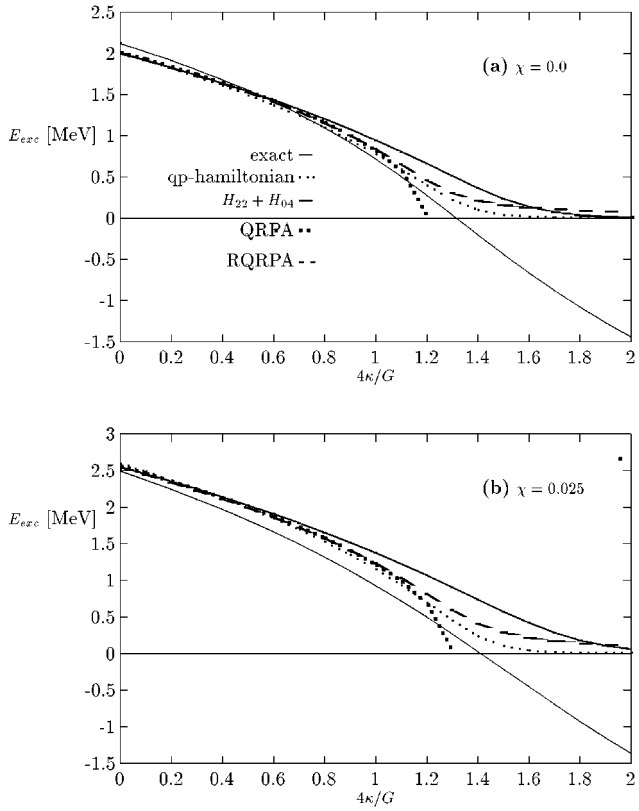

FIG. 5. (a) and (b): The same as Fig. 4(a) but for the excitation energy $E_{\rm exc}$ of the lowest 0^+ state in the odd-odd intermediate nucleus ($\mathcal{N}_n=13,\mathcal{N}_p=7$) with respect to the parent even-even nucleus ($\mathcal{N}_n=14,\mathcal{N}_p=6$), for $j=19/2$, $\chi=0$ (0.025).

$$v_i^2=\frac{1}{2}\left(1-\frac{e_i-Gv_i^2-\lambda_i}{\epsilon_i}\right), \quad i=p,n. \tag{14}$$

From this equation and from Eq. (12) the chemical potentials can be expressed as

$$\lambda_i=e_i-\frac{G\Omega}{2}+Gv_i^2, \quad i=p,n. \tag{15}$$

The excitation energy $E^{\lambda}_{\rm exc}$ of a state $|0_\lambda\rangle$ belonging to the spectrum of a double-odd-mass nucleus, with $\mathcal{N}_p+1$ protons and $\mathcal{N}_n-1$ neutrons, with respect to the ground state of the even-even neighbor with $\mathcal{N}_p,\mathcal{N}_n$, can easily be calculated if blocking is considered, i.e., when v_p,v_n are calculated for the even-even and odd-odd nuclei separately. These excitation energies are given by

$$E^{\lambda}_{\rm exc}=E(\lambda,\mathcal{N}_p+1,\mathcal{N}_n-1)-E({\rm g.s.},\mathcal{N}_n,\mathcal{N}_p)+\lambda_p-\lambda_n. \tag{16}$$

In the following we shall always refer to Eq. (16) as a suitable approximation for the excitation energies. In the present calculation we have selected e_p-e_n is such a way that

$$\lambda_p-\lambda_n=e_p-e_n-\frac{G}{2}(\mathcal{N}_n-\mathcal{N}_p)\frac{\Omega-1}{\Omega}=0, \tag{17}$$

which implies

$$e_p-e_n=\frac{G}{2}(\mathcal{N}_n-\mathcal{N}_p)\frac{\Omega-1}{\Omega}. \tag{18}$$

Alternatively, one can compute the occupation amplitudes v_p,v_n always for the even-even nucleus, without including blocking. The effect of blocking on the unperturbed excitation energies, with $\kappa=\chi=0$, can be ignored if the single-particle energy difference between protons and neutrons is modified to the value

$$e_p-e_n=\frac{G}{2}(\mathcal{N}_n-\mathcal{N}_p-1)\frac{\Omega-1}{\Omega}. \tag{19}$$

The linearized version of the Hamiltonian (11) is obtained by keeping only the first line of Eq. (11). This is equivalent to neglecting terms proportional to B and $B^\dagger$ (the so-called scattering terms). The solutions of this truncated Hamiltonian have been discussed in a previous paper [13].

Finding the eigenvalues and eigenvectors of the Hamiltonian (11) requires the use of the same algebraic techniques involved in solving the original Hamiltonian. However, the complexity of the problem increases severely due to the fact that neither the quasiparticle number or the quasiparticle isospin projection (or equivalently the number of proton and neutron quasiparticles) are good quantum numbers. It implies that the dimension of the basis will increase by 2 orders of magnitude. Additional reduced matrix elements would then be needed to diagonalize the Hamiltonian (11). The analytic expressions of these matrix elements are given in Appendix C.

There is a remaining symmetry in the Hamiltonian (11), since states with an even number of proton and neutron quasiparticles are not connected with states having an odd number of them. Due to this fact it is possible to separately diagonalize these two cases.

Particle number is not a good quantum number, obviously, because it is broken spontaneously by the Bogolyubov transformation. Thus, zero-quasiparticle states belonging the even-even-mass nucleus have good average number of protons and neutrons, the condition used to determine v_p,v_n, while states with a nonvanishing number of quasiparticles show strong fluctuations in the particle number. Fluctuations in the particle number can induce, naturally, important effects on the observables. Moreover, the admixture of several quasiparticle configurations in a given state, induced by residual particle-particle interactions, can also strongly influence the behavior of the observables. An example of this effect is given in [13], concerning the violation of the Ikeda sum rule produced by large values of the particle-particle strength κ.

The spectrum of the qp Hamiltonian (11) is shown in Figs. 4 and 5. The curves shown by small-dotted lines, in Figs. 4(a), 4(b), 5(a), and 5(b), display the dependence of the excitation energy for the qp Hamiltonian (11) upon the ratio κ/G. The results of this qp approximation closely follow the exact ones up to the point where they become negatives ($4\kappa/G\approx 1.4-1.8$ in the different cases). From this point on they vanish, rather than taking negative values, instead. The excitation energies for the linearized Hamiltonian $H_{22}+H_{04}$ are shown as thick lines in these figures. We can see that the linearized Hamiltonian is able to reproduce qualitatively the

behavior of the full qp one, but in general it overestimates the values of the excitation energies.

As is mentioned above, the results shown in Figs. 4 and 5 have been obtained both with the complete qp Hamiltonian and with the truncated Hamiltonian which includes only the product of pair-creation and annihilation operators. In [13] the relevance of the scattering terms in Eq. (11) was pointed out. From the present results it can be seen that the inclusion of these terms is indeed important if one looks after a better description of the qp-excitation energies, up to the point where the exact excitation energies become negative. For larger values of κ even the eigenstates of the complete Hamiltonian fail to describe negative excitation energies. This is a clear indication that other effects can play an important role, i.e., effects associated to the appearance of spurious states. This can be quantitatively illustrated by the following. There are four exact eigenstates for $j=19/2$, $\mathcal{N}_n=13$, $\mathcal{N}_p=7$, as can be seen in Fig. 2(a), while the spectrum of the qp Hamiltonian (11) has 220 eigenstates. It is well known that states with $\mathcal{N}_n=14\pm N_n$, $\mathcal{N}_p=6\pm N_p$, where N_p and N_n are the number of quasiparticle protons and neutrons, respectively, are mixed with two-$(p$-$n)$-quasiparticle states in the odd-odd nucleus and provide a large number of states belonging to other nuclei. When $4\kappa/G\ll 1$ the spurious states remain largely unmixed with the lower energy two-qp state. But when $4\kappa/G\approx 1$ the mixing becomes important. This fact upgrades the relevance of particle-number violation effects in dealing with this case.

The full qp-treatment represents the best possible extension of the quasiboson approximation, without performing a particle-number projection, in a single-j shell. It goes beyond any second extended RPA [27] and it includes explicitly all numbers of proton and neutron quasiparticles (N_p and N_n) in the eigenstates.

To analyze the effects associated to the number of quasiparticles in the ground state of double-even nuclei, and particularly the effects associated to the number of quasiprotons, we have calculated the average number of quasiprotons using the expression

$$\langle 0_\lambda|N_p|0_\lambda\rangle=\sum_{NTT_z}|C^{\lambda}_{NTT_z}|^2(N/2+T_z). \tag{20}$$

A similar expression holds for the average neutron-quasiparticle-number.

In Figs. 6(a) and 6(b) the average number of proton quasiparticles in the ground state of the even-even nucleus with $\mathcal{N}_p=6$, $\mathcal{N}_n=14$ is shown as a function of $4\kappa/G$, for $j=19/2$, $\chi=0$ and 0.04. Figures 7(a) and 7(b) show the number of proton quasiparticles for $\mathcal{N}_p=8$, $\mathcal{N}_n=12$, $j=19/2$, $\chi=0$ and 0.025. The dashed lines represent the results corresponding to the full qp Hamiltonian case while the large dots refer to the linearized $H_{22}+H_{04}$ version of it. The difference between both approximations is evident. Using the linearized Hamiltonian the states are composed only by proton-neutron-quasiparticle pairs [13], while the presence of the scattering terms introduces also like-$(p$-p and n-$n)$-quasiparticle pairs. The presence of these pairs, which for $4\kappa/G\approx 1$ play a crucial role, increases notably the number of quasiparticles and yields excitation energies closer to the exact ones.

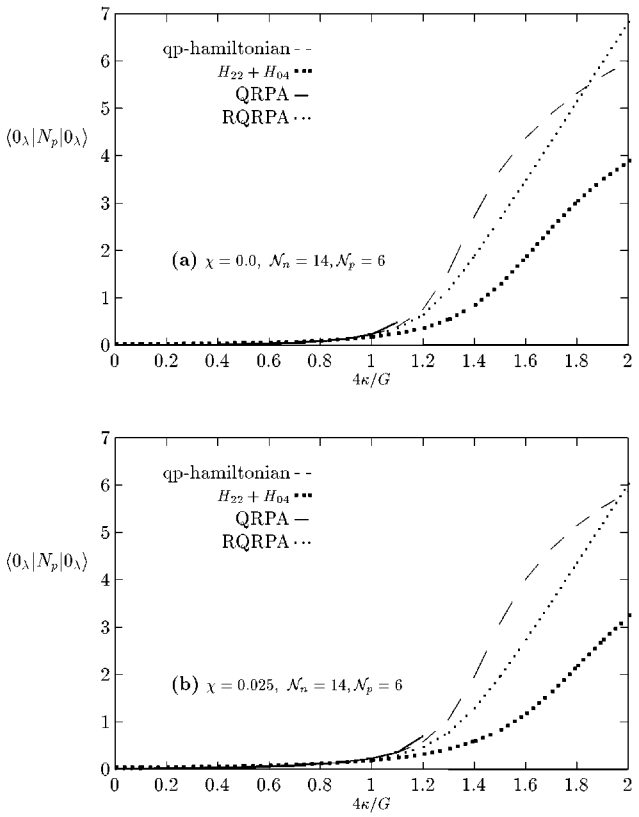

FIG. 6. (a) and (b): Average number of proton quasiparticles in the ground state of the even-even nucleus with $\mathcal{N}_p=6$, $\mathcal{N}_n=14$ as function of $4\kappa/G$, for $j=19/2$, $\chi=0$ (0.025) MeV. Results corresponding to the qp Hamiltonian are shown as dashed lines. The ones corresponding to the linearized qp Hamiltonian are shown as large-dotted lines and those of the QRPA and RQRPA methods as full lines and small-dotted lines, respectively.

The average quasiparticle number shows a saturation in the full-qp case for $4\kappa/G\approx 1.8$. At this value of the residual pn interaction the ground state is far away for the qp vacuum, and has a structure which can be described as a full quasiparticle shell. Notice that, at this point, the exact and full-qp excitation energies depart from each other. A state with four proton and four neutron quasiparticles has very large number fluctuations. Spurious states become strongly mixed with physical states. In this way the resulting excitation energies average to zero, a limit which differs from the exact value, which is negative.

The differences in the average qp number between full-qp and linearized approaches are larger in Figs. 6(a) and 6(b) than in Figs. 7(a) and 7(b). This result is a consequence of the dependence of some of the effective couplings of Eq. (11), i.e., $\lambda_3\approx u_p^2-v_p^2$ and $\lambda_4\approx u_n^2-v_n^2$, on the number of particles. As the number of particles approaches the saturation value $\Omega=(2j+1)/2$ the effective couplings λ_3 and λ_4 will vanish. Thus, the full-qp and linearized solutions yield similar results.

IV. QRPA AND RQRPA

The QRPA Hamiltonian H_{QRPA} can be obtained from the linearized version of Eq. (11), by keeping only the bilinear terms in the pair-creation and pair-annihilation operators.

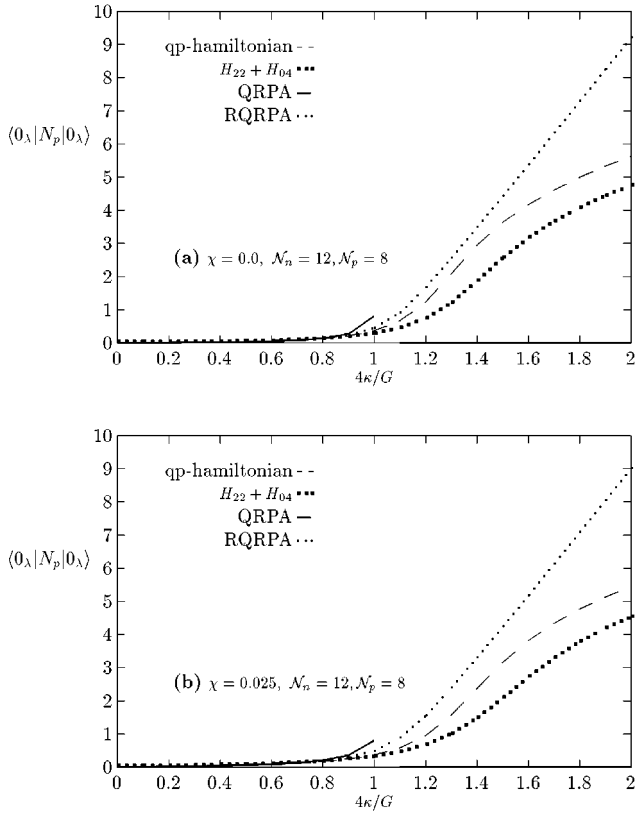

FIG. 7. (a) and (b): The same as Fig. 6 for the number of proton quasiparticles for $\mathcal{N}_p=8, \mathcal{N}_n=12,\ j=19/2,\ \chi=0$ (0.025) MeV.

The pair-creation and pair-annihilation operators, $A^\dagger$ and A, are, of course, defined by coupled pairs of fermions. The commutation relations between these pseudoboson operators include numberlike quasiparticle operators in addition to unity. By taking the limit $(2j+1)\to\infty$ [13] these extra terms vanish and the commutation relations between pairs of fermions can be treated like exact commutation relations between bosons. This is the well-known quasiboson approximation and the QRPA Hamiltonian is the leading order Hamiltonian which satisfies the quasiboson approximation. If the pair operators are replaced by quasibosons, the resulting Hamiltonian is given by

$$H_{\mathrm{QRPA}}=(2\epsilon+\lambda_1)b^\dagger b+\lambda_2\{b^\dagger b^\dagger+bb\}. \tag{21}$$

As said above, the quasibosons $b^\dagger$ and b fulfill exactly the commutation relation $[b,b^\dagger]=1$.

At this point we can refer to pair of fermions ($A^\dagger$) or to quasibosons ($b^\dagger$) without lost of generality, since we have not introduced a particular representation for the pair of fermions to boson mapping.

The QRPA states are generated by the action of the one-phonon operator $O^\dagger_{\mathrm{QRPA}}=XA^\dagger-YA$ on the correlated QRPA vacuum $|0\rangle$. The quasiboson approximation assumes that $\langle 0|[A,A^\dagger]|0\rangle=1$ and it leads to the normalization condition $X^2-Y^2=1$. The QRPA matrix is just a 2×2 one, with submatrices $\mathcal{A}_{\mathcal{QRPA}}=2\epsilon+\lambda_1$ and $\mathcal{B}_{\mathcal{QRPA}}=2\lambda_2$. The corresponding eigenvalue is given by $E_{\mathrm{QRPA}}=[(2\epsilon+\lambda_1)^2-4\lambda_2^2]^{1/2}$. It becomes purely imaginary if $2\lambda_2>2\epsilon+\lambda_1$.

For this limit the backward-going amplitudes of the QRPA phonon operator become dominant, thus invalidating the underlying assumption about the smallness of the quasiboson vacuum amplitudes. The QRPA excitation energies, obtained with the above-introduced Hamiltonian are shown in Figs. 4 and 5. It can be seen that in the four cases displayed in these figures the collapse of the QRPA values occurs near the point where the exact excitation energies become negative. This is a very important result because it means that the QRPA description of the dynamics given by the Hamiltonian (1) is able to reproduce exact results. At this point one can naturally ask the obvious question about the nature of the mechanism which produces such a collapse. The fact that the QRPA approximation is sensitive to it, together with the fact that the same behavior is shown by the exact solution, reinforces the idea about the onset of correlations which terminate the regime of validity of the pair-dominant picture. In order to identify such correlations we have calculated the expectation value of the number of quasifermions and bosons on the QRPA ground state.

The average number of proton quasiparticles in the QRPA ground state, which in this case coincides with the average boson number, is given by[1]

$$\langle 0|N_p|0\rangle=Y^2. \tag{22}$$

Figures 6(a), 6(b), 7(a), and 7(b) show the results corresponding to these occupation numbers. The QRPA results extend up to the value $4\kappa/G\approx1$, where the QRPA collapses. The sudden increase of the average quasiparticle number near the collapse of the QRPA is a clear evidence about a change in the structure of the QRPA ground state.

In the renormalized QRPA the structure of the ground state is included explicitly [9] in the form

$$|0\rangle=\mathcal{N}e^S|\mathrm{BCS}\rangle,\quad S=\frac{cA^\dagger A^\dagger}{2\langle 0|[A,A^\dagger]|0\rangle}, \tag{23}$$

where the quasiboson approximation, at the commutator's level, is not enforced explicitly. The renormalization procedure consists of retaining approximately the number of quasiparticle-like terms of the commutators keeping them as a parameter to be determined, namely, by defining the RQRPA one-phonon state as

$$O^\dagger_{\mathrm{RQRPA}}|0\rangle=[\mathcal{X}A^\dagger-\mathcal{Y}A]/\langle 0|[A,A^\dagger]|0\rangle^{1/2}|0\rangle \tag{24}$$

and enforcing the condition $O_{\mathrm{RQRPA}}|0\rangle=0$, which leads to the estimate $c=\mathcal{Y}/\mathcal{X}$ for the parameter entering in the definition of the correlated vacuum. After some algebra it is possible to show that $\langle 0|[A,A^\dagger]|0\rangle\equiv D=1-[2\mathcal{Y}^2D/(2j+1)]$ [10,11], and that

$$D=\left[1+\frac{2\mathcal{Y}^2}{2j+1}\right]^{-1}. \tag{25}$$

The RQRPA submatrices are $\mathcal{A}_{\mathcal{RQRPA}}=2\epsilon+\lambda_1D$ and $\mathcal{B}_{\mathcal{RQRPA}}=2\lambda_2D$. Since $0\leqslant D\leqslant1$, the presence of D multiplying both λ_1 and λ_2 produces the reduction of the residual interaction which is needed to avoid the collapse of the QRPA equations [11]. Due to this fact, the RQRPA energy

[1]Notice that there is a factor 2 misprinted in Eq. (19) of [13].

E_{RQRPA} is always real. Its value can be obtained by solving simultaneously the nonlinear equations for $E_{\mathrm{RQRPA}}, \mathcal{X}, \mathcal{Y}$, and D, which in the general case will include all possible values of the multipolarity J [11].

RQRPA excitation energies are shown in Figs. 4 and 5. These results strongly resemble those of Fig. 1 of [11] and Fig. 2 of [6]. The results corresponding to the QRPA (of [6]) and to the RQRPA (of [11]) are quite similar to those shown in Figs. 4 and 5. However, the main finding of the present calculations is that the exact excitation energies are closer to the QRPA energies, rather than to the renormalized ones, instead. In exact calculations including the spin degrees of freedom a phase transition was found at the point where the QRPA collapses [28], thus reinforcing the present results.

The average number of quasiparticles in the RQRPA vacuum is given by

$$\langle 0|N_p|0\rangle = \mathcal{Y}^2, \tag{26}$$

and it is shown in Figs. 6(a), 6(b), 7(a), and 7(b). It is fairly obvious from these results that the RQRPA ground-state correlations double in all cases of the complete solutions of the linearized Hamiltonian. This is clearly an overestimation, and it is probably one of the most notorious difficulties confronting the use of the RQRPA.

It allows too many ground-state correlations, and with them the particle-number fluctuations are introducing spurious states which can dominate the low-energy structure for large values of κ.

Near ''collapse'' the average number of quasiparticles given by the QRPA and the RQRPA are comparable. For the case of the QRPA the increase of the ground-state correlations is determined by the change in the sign of the backward-going matrix relative to the forward-going one near collapse. From there on the QRPA cannot produce any physically acceptable result since one of the underlying conditions of the approximation, i.e., the positive definite character of either linear combination of the forward- and backward-going blocks of the QRPA matrix will not be fulfilled. This collapse is prevented in the RQRPA, by the use of the renormalization of the matrix elements, but the drawback of the approximation is the contribution coming from spurious states, which ought to be removed. Moreover, there are several other reasons to cast doubts on the consistency of the RQRPA. Among them, the mixing up of orders in the wave functions, of the RQRPA phonons, is not accompanied by the enlargement of the Hamiltonian, to accommodate other correlations, i.e., the exchange terms of the QRPA matrix. If one performs such a calculation, by including exchange terms, the resulting values of the QRPA matrix terms are also ''renormalized,'' but this effect will depend upon the configurations. Also, the point of collapse is shifted to higher values of the coupling constant κ but the effect is typically of the order $1/\Omega$, as compared to leading order terms. If terms others than unity are introduced in the commutators, then the Hamiltonian has to be enlarged to account for the AB sort of terms of the initial Hamiltonian, see Eq. (11), because they will contribute at the same order as the added number-type of terms introduced by the RQRPA procedure. Thus, the RQRPA procedure should be accompanied by a renormalization of the transition operators and/or by the inclusion of scattering terms also in these operators. At this level, by going beyond the leading order QRPA approximation, more terms have to be added to the diagrams which represent the transition amplitudes. It has been done for a pure seniority model in [29]. This approach, for correlations between pairs of like quasiparticles, is already cumbersome and it introduces an unmanageable number of contributions, both to the QRPA matrix as well as to the transition operators. For unlike pairs of quasiparticles the situation can be even worse, since the complete algebra, which supports the expansions, cannot be defined in a subspace where scattering terms are replaced by c numbers. More details about these aspects will be presented in a forthcoming publication.

V. DOUBLE BETA DECAY

In this section we shall briefly discuss some of the consequences of the previously presented approaches on the calculation of nuclear double-beta decay observables. In the following we shall focus our attention on the two-neutrino mode of the nuclear double-beta decay, since the matrix elements governing this decay mode are more sensitive to nuclear structure effects than the ones of the neutrinoless mode. As said in the Introduction we shall consider only double-Fermi transitions. The nuclear matrix elements of the two-neutrino double-beta decay $M_{2\nu}$ can be written as

$$M_{2\nu} = \sum_{\lambda} \frac{\langle 0_f|\beta^-|0_\lambda\rangle\langle 0_\lambda|\beta^-|0_i\rangle}{E_\lambda - E_i + \Delta}, \tag{27}$$

where $|0_i\rangle, |0_\lambda\rangle$, and $|0_f\rangle$ represent the initial, intermediate, and final nuclear states participant of the virtual transitions entering in the allowed second-order weak processes. The energies of the initial and intermediate states are E_i and E_λ, respectively. The energy released by the decay is represented by the quantity Δ. For the present calculations we have selected the value of $\Delta = 0.5$ MeV, which is of the order of magnitude of the empirical values used in realistic calculations. The results for the matrix elements $M_{2\nu}$ obtained with the exact wave functions are shown as a function of the ratio $4\kappa/G$ in Figs. 8(a) and 8(b). These results have been obtained with the following set of parameters: $j = 9/2 (\mathcal{N}_p = 2,\ \mathcal{N}_n = 8) \rightarrow (\mathcal{N}_p = 4,\ \mathcal{N}_n = 6)$, and $\chi = 0$ and 0.04 MeV, respectively. The values shown in Figs. 9(a) and 9(b) correspond to $j = 19/2, (\mathcal{N}_p = 6,\ \mathcal{N}_n = 14) \rightarrow (\mathcal{N}_p = 8,\ \mathcal{N}_n = 12)$, and $\chi = 0$ and 0.025 MeV.

For all cases the exact value of $M_{2\nu}$ vanishes at the point $4\kappa/G = 1$. As mentioned above, this cancellation appears in the model due to the fact that, for this value of κ, the isospin symmetry is recovered and the ground states of the initial and final nuclei belong to different isospin multiplets, as can be seen also from the results shown in Figs. 1 and 2.

A similar mechanism, in the context of a solvable model possessing an SO(8) algebra including spin and isospin degrees of freedom, was used a decade ago to show that the cancellation of the $M_{2\nu}$ matrix elements for certain values of the particle-particle residual interaction was not an artifact of the QRPA description [2].

The results corresponding to the matrix elements $M_{2\nu}$, calculated with the different approximations discussed in the text, are shown in Figs. 8 and 9, as a function of the coupling

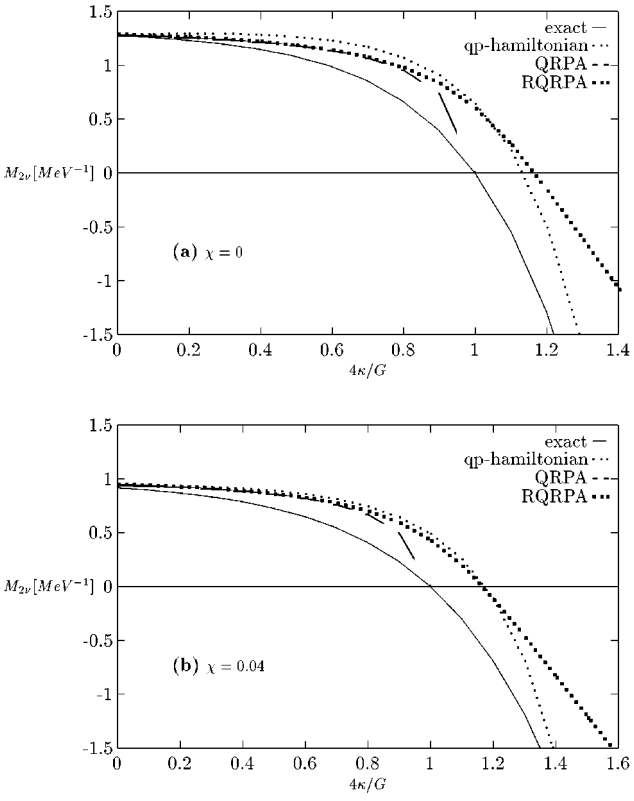

FIG. 8. (a) and (b): Matrix elements $M_{2\nu}$ for the double-Fermi two-neutrino double-beta decay mode, as functions of the ratio $4\kappa/G$ for $j=9/2,(\mathcal{N}_p=2,\mathcal{N}_n=8)\rightarrow(\mathcal{N}_p=4,\mathcal{N}_n=6)$, and $\chi=0$ (0.04) MeV. Exact results are indicated by thin-full lines. The results obtained with the qp Hamiltonian are shown as small-dotted lines and the results of the QRPA and RQRPA methods as dashed lines and large-dotted lines, respectively.

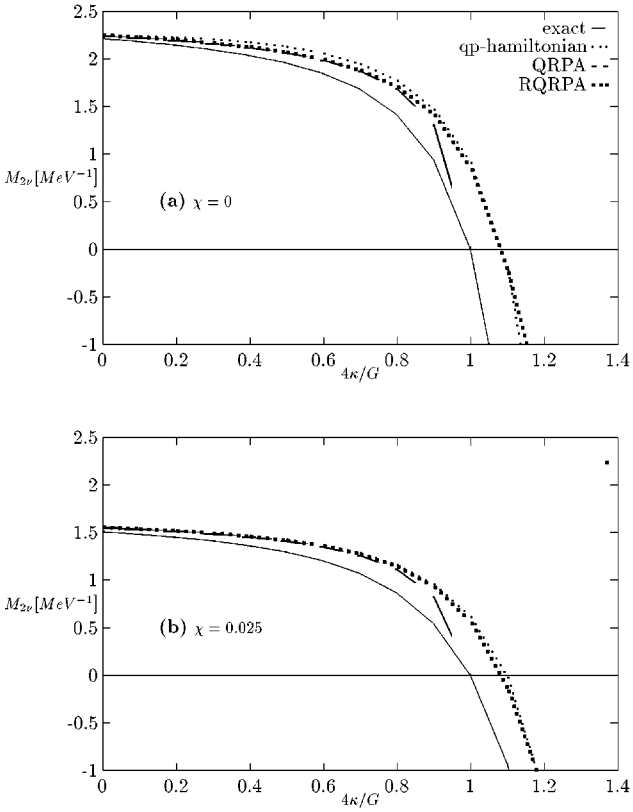

FIG. 9. (a) and (b): The same as Fig. 8, i.e., the matrix elements $M_{2\nu}$, for $j=19/2,(\mathcal{N}_p=6,\mathcal{N}_n=14)\rightarrow(\mathcal{N}_p=8,\mathcal{N}_n=12)$, and $\chi=0$ (0.025) MeV.

constant κ. The values of $M_{2\nu}$ are very similar to those found in realistic calculations [1,3,4,11], including its strong suppression for values of the coupling constant κ near the value which produces the collapse of the QRPA description. Distinctively, the RQRPA results extend to values of κ passing the ''critical'' value. However, the validity of this result can be questioned because, as we have shown above, the RQRPA missed the vanishing of the excitation energy. The $M_{2\nu}$ matrix elements, evaluated with the complete qp Hamiltonian (11), are quite similar to that of the RQRPA up to point where it vanishes. From this point on the results of both the full-qp and the RQRPA approximations are different. Both matrix elements change their sign at a value of κ which is larger than the one corresponding to the change of the sign of the matrix elements calculated with the exact wave function. The fact that the RQRPA results and the ones of the qp approximation are similar, although these models differ drastically in the correlations which they actually include, suggest that a kind of balance is established between terms which are responsible for ground-state correlations and those which produce the breaking of coherence in the wave functions. Obviously this mechanism must be related to the presence of scattering terms in the commutators as well as in the Hamiltonian.

VI. CONCLUSIONS

An exactly solvable model for the description of single- and double-beta decay processes of the Fermi type was introduced. The model is equivalent to a complete shell-model treatment in a single-j shell for the adopted Hamiltonian. It reproduces the main features of the results obtained in realistic calculations, with many shell and effective residual interactions, like those used in the literature to describe the microscopic structure of the nuclei involved in double-beta decay processes.

We have constructed the exact spectrum of the Hamiltonian and discussed its properties. The results concerning the energy of the states belonging to the exact solution of the model show that, in spite of its very schematic structure, the Hamiltonian is able to qualitatively reproduce the nuclear mass parabola. The sequence of levels of the exact solution shows that the ground state and the first excited state, of the spectrum of double-even nuclei, approach a band-crossing situation for a critical value of the strength associated with attractive particle-particle interactions. At the crossing these states interchange their quantum numbers. This behavior is connected with the description of ''shape'' transitions in similar theories, where the order parameter is clearly associated with multipole deformations in r space. In the present model the ''deformation'' mechanism is related with the breaking of the isospin symmetry and the space rotation corresponds to a rotation in isospin space which preserves the third component of the isospin.

We have compared the exact values of the excitation energy and of the double-beta decay matrix elements, for double-Fermi transitions, with those obtained by using the solutions of the approximate qp Hamiltonian, its linearized version, and both the QRPA and RQRPA ones.

It was shown that the collapse of the QRPA correlates with the presence of an exact eigenvalue at zero energy. The structure of the RQRPA solutions has been discussed and it was found that, although finite, they are not free from spurious contributions. The role of scattering terms was discussed and they were shown to be relevant in getting excitation energies closer to the exact values. However they are not enough to generate the correlations which are needed to produce the band crossing or negative excitation energies as it was found in the exact solution for large values of the coupling constant κ.

In order to correlate the breakup of the QRPA approximation with the onset of strong fluctuations in the particle number we have calculated the average number of quasiparticles in the different approximations discussed in the text.

It was shown that the solutions of the complete qp Hamiltonian display a strong change in the structure of the ground state when the particle-particle strength increases. The qp content of the ground state varies from a nearly zero value to an almost full qp occupancy. The particle number fluctuations associated with states with a large number of quasiparticles were mentioned as a possible source of spurious states.

Double-beta decay amplitudes were evaluated in the different formalisms. Their similitudes and differences were pointed out.

As a conclusion, the need of additional work to clarify the meaning of the different approximations posed by the RQRPA was pointed out.

ACKNOWLEDGMENTS

Partial support of the Conacyt of Mexico and the CONICET of Argentina is acknowledged. One of the authors (O.C.) gratefully acknowledges a grant of the J. S. Guggenheim Memorial Foundation.

APPENDIX A: THE SO(5) ALGEBRA

Following [20] we introduce the operators

$$A^\dagger(0)\equiv[\alpha_p^\dagger\otimes\alpha_n^\dagger]^{J=0}_{M=0}=A^\dagger,$$

$$A^\dagger(1)\equiv\frac{1}{\sqrt{2}}[\alpha_n^\dagger\otimes\alpha_n^\dagger]^{J=0}_{M=0},\quad A^\dagger(-1)\equiv\frac{1}{\sqrt{2}}[\alpha_p^\dagger\otimes\alpha_p^\dagger]^{J=0}_{M=0},\tag{A1}$$

$$B^\dagger=[\alpha_p^\dagger\otimes\alpha_n^\dagger]^{J=0}_{M=0},\quad T^-=-\sqrt{2\Omega}B^\dagger,$$

which together with their Hermitian conjugates and with the number and isospin operators

$$N=N_p+N_n,\quad T_z=\frac{N_p-N_n}{2},$$

$$N_i=\sum_{m_i}\alpha^\dagger_{im_i}\alpha_{im_i},\quad i=p,n,\tag{A2}$$

are the ten generators of the SO(5) group.

The Hermitian conjugates of the pair-creation operators transform, under isospin reversal, as

$$\tilde{A}(M)\equiv(-1)^M A(-M).\tag{A3}$$

Their commutation relations are more easily expressed defining the new operators

$$H_1=\frac{N}{2}-\Omega,\quad H_2=T_z,$$

$$E_{11}=\sqrt{\Omega}A^\dagger(1),\quad E_{-1-1}=\sqrt{\Omega}A(1),$$

$$E_{1-1}=-\sqrt{\Omega}A^\dagger(-1),\quad E_{-11}=-\sqrt{\Omega}A(-1),\tag{A4}$$

$$E_{10}=\sqrt{\Omega}A^\dagger(0),\quad E_{-10}=\sqrt{\Omega}A(0),$$

$$E_{01}=\frac{1}{\sqrt{2}}T^+,\quad E_{0-1}=\frac{1}{\sqrt{2}}T^-.$$

The operators $E_{\alpha\beta}$ are raising and lowering operators. When operating on an eigenstate of the weight operators H_1 and H_2 they increase or decrease the eigenvalues of one or both by one unit. Their commutation relations are

$$[H_1,H_2]=0,\quad [H_1,E_{\alpha\beta}]=\alpha E_{\alpha\beta},\quad [H_2,E_{\alpha\beta}]=\beta E_{\alpha\beta},$$

$$[E_{\alpha\beta},E_{-\alpha-\beta}]=\alpha H_1+\beta H_2,\tag{A5}$$

$$[E_{\alpha\beta},E_{\alpha'\beta'}]=\begin{cases}\pm E_{\alpha+\alpha'\beta+\beta'} & \text{if } \alpha+\alpha' \text{ and } \beta+\beta'=0,1,-1,\\ 0 & \text{otherwise.}\end{cases}$$

More explicitly

$$[E_{11},E_{-10}]=E_{01},\quad [E_{11},E_{0-1}]=-E_{10},$$

$$[E_{10},E_{-11}]=-E_{01},$$

$$[E_{10},E_{-1-1}]=E_{0-1},\quad [E_{10},E_{01}]=-E_{11},$$

$$[E_{10},E_{0-1}]=E_{1-1},\tag{A6}$$

$$[E_{1-1},E_{-10}]=-E_{0-1},\quad [E_{1-1},E_{01}]=E_{10},$$

and by Hermitian conjugation of the above commutators one obtains

$$E^\dagger_{\alpha\beta}=E_{-\alpha-\beta}.\tag{A7}$$

APPENDIX B: SO(5) REPRESENTATIONS

The highest weights of the operators H_1,H_2 define the irreducible representations (irrep) of the SO(5) algebra. For the present case we want the irrep which contains the state with zero quasiparticles as well as the state completely filled with quasiproton and quasineutrons. The maximum number ($N_{\max}$) of quasiparticles allowed by the Pauli principle is 2Ω, thus adding quasiprotons and quasineutrons one obtains $N_{\max}=4\Omega$. This is the state with the highest weight and it

belongs to the irrep defined by $(H_1=\Omega,H_2=0)$ or $N=4\Omega,T=T_z=0$. Acting with the generators (A2) on this state it is possible to generate the set of all the states with an even number of quasiparticles. This subspace suffices for all the calculations described in this work. For this reason we have adopted the irrep $(H_1=\Omega,H_2=0)$.

In general it is necessary to specify four quantum numbers to completely define a state in a given irrep. But for the present case it turns out that the states can be defined by the quantum numbers N,T,T_z.

In the following we will construct explicitly the states $|NTT_z=T\rangle$; other states with $T_z\neq T$ are obtained by acting with the isospin lowering operator T^- on them. The states of this basis are defined by

$$|NT=T_z\rangle=N(a,b)(O_{00})^b(O_+)^a|N=4\Omega T=T_z=0\rangle,$$

where

$$O_+=E_{-11},\quad O_{00}=2E_{-11}E_{-1-1}+E_{-10}E_{-10},\quad \text{(B1)}$$

$$a=T_z=T,\quad b=\Omega-\frac{T}{2}-\frac{N}{4},$$

$$N(a,b)=2^b\left[\frac{(2\Omega+1-2b)!(\Omega-a-b)!(2a+1)!(a+b)!}{(2\Omega+1)!(\Omega-b)!(a!)^2b!(2a+2b+1)!}\right]^{1/2}.$$

APPENDIX C: SO(5) REDUCED MATRIX ELEMENTS

To diagonalize the Hamiltonian (11) in the (N,T,T_z) basis, or the Hamiltonian (1) in the $\mathcal{N},\mathcal{T},\mathcal{T}_z$ basis, requires the use of the Wigner-Eckart theorem

$$\langle N'T'T'_z|O^{ntt_z}|NTT_z\rangle=(TT_z,tt_z|T'T'_z)\langle N'T'||O^{nt}||NT\rangle, \quad \text{(C1)}$$

where on the right-hand side the symbol $(..,..|..)$ represents a Clebsch-Gordan coefficient and $\langle..||[..]||..\rangle$ is a reduced matrix element. Explicit expressions for the reduced matrix elements are given below. The difference in the number of creation and annihilation operators in the tensor O is represented by n and in order to obtain nonzero matrix elements it must be equal to $N'-N$.

We have used of the Wigner-Eckart theorem, the commutation relations given in Appendix A, and the explicit form of the states with $T=T_z$ shown in Appendix B to calculate the reduced matrix elements of the different operators which are relevant in our problem. Some of these SO(5)-reduced matrix elements are listed here. Additional matrix elements can be deduced from them by using

$$\langle NT||(O^{nt})^\dagger||N'T'\rangle=\sqrt{\frac{2T'+1}{2T+1}}\langle N'T'||O^{nt}||NT\rangle. \quad \text{(C2)}$$

The relevant reduced matrix elements are

$$\langle N\ \ T+2||[A^\dagger\tilde{A}]^{t=2}||NT\rangle=\frac{-1}{2\Omega}\left[\frac{(2\Omega-T-N/2)(T+N/2+3)(-T+N/2)(2\Omega+T-N/2+3)(T+1)(T+2)}{(2T+3)(2T+5)}\right]^{1/2},$$

$$\langle NT||[A^\dagger\tilde{A}]^{t=0}||NT\rangle=\frac{1}{2\sqrt{3}\Omega}[(2\Omega-N/2+3)N/2-T(T+1)],$$

$$\langle NT||[A^\dagger\tilde{A}]^{t=2}||NT\rangle=\frac{1}{\sqrt{6}(TT,20|TT)}[\langle NT=T_z|A^\dagger(1)A(1)|NT=T_z\rangle+\langle NT=T_z|A^\dagger(-1)A(-1)|NT=T_z\rangle$$
$$-2\langle NT=T_z|A^\dagger(0)A(0)|NT=T_z\rangle],$$

where

$$\langle NT=T_z|A^\dagger(1)A(1)|NT=T_z\rangle=\frac{1}{\Omega}\left[-\Omega+T+N/2+\frac{(2\Omega-T-N/2)(T+N/2+3)(T+1)}{2(2T+3)}\right],$$

$$\langle NT=T_z|A^\dagger(-1)A(-1)|NT=T_z\rangle=\frac{1}{\Omega}\left[\frac{(2\Omega-T-N/2+3)(-T+N/2)(T+1)}{2(2T+3)}\right],$$

$$\langle NT=T_z|A^\dagger(0)A(0)|NT=T_z\rangle=\frac{1}{\Omega}\left[-\Omega+N/2+\frac{(2\Omega-T-N/2)(T+N/2+3)\Omega}{(2\Omega+T-N/2+1)(-T+N/2+2)}\langle N+4T=T_z|A^\dagger(0)A(0)|N+4T=T_z\rangle\right].$$

The largest value that N can take is $4\Omega-2T$. In this case

$$\langle N=4\Omega-2TT=T_z|A^\dagger(0)A(0)|N=4\Omega-2TT=T_z\rangle=1-T/\Omega.$$

The above-reduced matrix elements are enough to deal with the Hamiltonian (1), which conserves particle number. Working with the Hamiltonian (11) requires many other reduced matrix elements, like the following matrix elements:

$$\langle N+4T||[A^\dagger A^\dagger]^{t=0}||NT\rangle=\frac{-1}{2\sqrt{3}\Omega}[(T+N/2+3)(-T+N/2+2)(2\Omega-T-N/2)(2\Omega+T-N/2+1)]^{1/2},$$

$$\langle N+4T-2||[A^\dagger A^\dagger]^{t=2}||NT\rangle=\frac{1}{2\Omega}\left[\frac{(-T+N/2+4)(-T+N/2+2)(T-1)T(2\Omega+T-N/2-1)(2\Omega+T-N/2+1)}{(2T-1)(2T-3)}\right]^{1/2},$$

$$\langle N+4T+2||[A^\dagger A^\dagger]^{t=2}||NT\rangle=\frac{1}{2\Omega}\left[\frac{(T+N/2+3)(T+N/2+5)(T+1)(T+2)(2\Omega-T-N/2)(2\Omega-T-N/2-2)}{(2T+3)(2T+5)}\right]^{1/2},$$

$$\langle N+2T-1||A^\dagger||NT\rangle=-\left[\frac{T(-T+N/2+2)(2\Omega+T-N/2+1)}{2\Omega(2T-1)}\right]^{1/2},$$

$$\langle N+2T+1||A^\dagger||NT\rangle=\left[\frac{(T+1)(T+N/2+3)(2\Omega-T-N/2)}{2\Omega(2T+3)}\right]^{1/2}.$$

These matrix elements, together with those associated with the isospin raising and lowering operators

$$T^+=-\sqrt{2\Omega}B,\quad T^-=-\sqrt{2\Omega}B^\dagger,$$

$$\langle NTT_z+1|B|NTT_z\rangle=-[(T+T_z+1)(T-T_z)]^{1/2}/\sqrt{2\Omega},$$

$$\langle NTT_z-1|B^\dagger|NTT_z\rangle=-[(T-T_z+1)(T+T_z)]^{1/2}/\sqrt{2\Omega},$$

are all the elements which are needed to diagonalize the Hamiltonian (11) and to calculate the matrix elements of the transition operators.

[1] P. Vogel and M. R. Zirnbauer, Phys. Rev. Lett. **57**, 3148 (1986).
[2] J. Engel, P. Vogel, and M. R. Zirnbauer, Phys. Rev. C **37**, 731 (1988).
[3] O. Civitarese, A. Faessler, and T. Tomoda, Phys. Lett. B **194**, 11 (1987).
[4] K. Muto, E. Bender, and H. V. Klapdor, Z. Phys. A **334**, 177 (1989).
[5] O. Civitarese, A. Faessler, J. Suhonen, and X. R. Wu, Nucl. Phys. **A524**, 404 (1991).
[6] O. Civitarese, A. Faessler, J. Suhonen, and X. R. Wu, J. Phys. G **17**, 943 (1991).
[7] A. Griffiths and P. Vogel, Phys. Rev. C **46**, 181 (1992).
[8] K. Hara, Prog. Theor. Phys. **32**, 88 (1964); K. Ikeda, T. Udagawa, and Y. Yamaura, *ibid.* **33**, 22 (1965).
[9] D. J. Rowe, Phys. Rev. **175**, 1283 (1968); Rev. Mod. Phys. **40**, 153 (1968); J. C. Parick and D. J. Rowe, Phys. Rev. **175**, 1293 (1968); D. J. Rowe, Nucl. Phys. **A107**, 99 (1968).
[10] F. Catara, N. Dinh Dang, and M. Sambataro, Nucl. Phys. **A579**, 1 (1994).
[11] J. Toivanen and J. Suhonen, Phys. Rev. Lett. **75**, 410 (1995).
[12] J. Schwieger, F. Simkovic, and Amand Faessler, Nucl. Phys. **A600**, 179 (1996).
[13] J. G. Hirsch, P. O. Hess, and O. Civitarese, Phys. Rev. C **54**, 1976 (1996).
[14] J. G. Hirsch, P. O. Hess, and O. Civitarese, Phys. Lett. B **390**, 36 (1997).
[15] V. A. Kuz'min and V. G. Soloviev, Nucl. Phys. **A486**, 118 (1988).
[16] K. Muto, E. Bender, T. Oda, and H. V. Klapdor-Kleingrothaus, Z. Phys. A **341**, 407 (1992).
[17] O. Civitarese and J. Suhonen, J. Phys. G **20**, 1441 (1994).
[18] O. Civitarese and J. Suhonen, Nucl. Phys. **A578**, 62 (1994).
[19] O. Civitarese, J. Suhonen, and Amand Faessler, Nucl. Phys. **A591**, 195 (1995).
[20] J. C. Parikh, Nucl. Phys. **63**, 214 (1965).
[21] K. T. Hecht, Nucl. Phys. **63**, 177 (1965).
[22] A. Klein and E. R. Marshalek, Rev. Mod. Phys. **63**, 375 (1991).
[23] L. S. Kisslinger and R. A. Sorensen, Rev. Mod. Phys. **35**, 853 (1963).
[24] D. Agassi, Nucl. Phys. **A116**, 49 (1968).
[25] D. Schütte and K. Bleuler, Nucl. Phys. **A119**, 221 (1968).
[26] D. J. Rowe, *Nuclear Collective Motion* (Methuen and Co. Ltd., London, 1970).
[27] A. Mariano, J. Hirsch, and F. Krmpotić, Nucl. Phys. **A518**, 523 (1990), and references therein.
[28] J. Engel, S. Pittel, M. Stoitsov, P. Vogel, and J. Dukelsky, Phys. Rev. C **55**, 1781 (1997).
[29] J. Dukelsky and P. Schuck, Phys. Lett. B **387**, 233 (1996).